

University of Montana

## ScholarWorks at University of Montana

---

Graduate Student Theses, Dissertations, &  
Professional Papers

Graduate School

---

2019

### Assessing the Robustness of Time-to-Event Abundance Estimation

Kenneth E. Loonam  
*University of Montana, Missoula*

Follow this and additional works at: <https://scholarworks.umt.edu/etd>



Part of the [Population Biology Commons](#)

Let us know how access to this document benefits you.

---

#### Recommended Citation

Loonam, Kenneth E., "Assessing the Robustness of Time-to-Event Abundance Estimation" (2019).  
*Graduate Student Theses, Dissertations, & Professional Papers*. 11477.  
<https://scholarworks.umt.edu/etd/11477>

This Thesis is brought to you for free and open access by the Graduate School at ScholarWorks at University of Montana. It has been accepted for inclusion in Graduate Student Theses, Dissertations, & Professional Papers by an authorized administrator of ScholarWorks at University of Montana. For more information, please contact [scholarworks@mso.umt.edu](mailto:scholarworks@mso.umt.edu).

ASSESSING THE ROBUSTNESS OF TIME-TO-EVENT ABUNDANCE ESTIMATION

By

KENNETH EDWARD LOONAM

Bachelor of Science, Texas A&M University, College Station, TX, 2012

Thesis

presented in partial fulfillment of the requirements  
for the degree of

Master of Science  
in Wildlife Biology

The University of Montana  
Missoula, MT

December 2019

Approved by:

Scott Whittenburg, Dean of The Graduate School  
Graduate School

Dr. Hugh S. Robinson, Co-Chair  
Panthera, Wildlife Biology Program, Department of Ecosystem and Conservation Sciences

Dr. Michael S. Mitchell, Co-Chair  
Wildlife Biology Program, Montana Cooperative Wildlife Resource Unit

Dr. Paul M. Lukacs  
Wildlife Biology Program, Department of Ecosystem and Conservation Sciences

Dr. David Ausband  
University of Idaho, Idaho Cooperative Wildlife Research Unit  
Idaho Department of Fish and Game

Assessing the Robustness of Time-to-Event Abundance Estimation

Chairperson: Hugh S. Robinson

**ABSTRACT**

Abundance estimates can inform management policies and are used to address a variety of wildlife research questions, but reliable estimates of abundance can be difficult and expensive to obtain. For low-density, difficult to detect species, such as cougars (*Puma concolor*), the costs and intensive field effort required to estimate abundance can make working at broad spatial and temporal scales impractical. Remote cameras have proven effective in detecting these species, but the widely applied methods of estimating abundance from remote cameras rely on some portion of the population being marked or uniquely identifiable, limiting their utility to populations with naturally occurring marks and populations that have been collared or tagged. Methods to estimate the abundance of unmarked populations with remote cameras have been proposed, but none have been widely adopted due, in part, to difficulties meeting the model assumptions. I examined the robustness of one model for estimating abundance of unmarked populations, the time-to-event model, to violating assumptions using walk simulations. I also tested the robustness of the time-to-event model to the low sample sizes of species that live at low densities by applying it alongside genetic spatial capture recapture on two populations of cougars (*Puma concolor*) in Idaho, USA. The time-to-event model is robust to many potential violations of assumptions but biased by incorrectly estimating movement speed and non-random sampling. The time-to-event model can effectively estimate the density of species living at low density and was more precise than and as reliable as genetic spatial capture recapture. Camera based abundance estimates that do not require individual identification, such as the time-to-event model, solve many of the challenges of monitoring low-density, difficult to detect species and make broad scale, multi-species monitoring more feasible.

## TABLE OF CONTENTS

Abstract .....	ii
Acknowledgements .....	iv
Chapter 1 .....	1
Introduction .....	1
Methods .....	5
Results .....	11
Discussion .....	13
Figure .....	16
Literature Cited .....	19
Chapter 2 .....	22
Introduction .....	22
Methods .....	24
Results .....	29
Discussion .....	30
Figures .....	34
Literature Cited .....	37

## **Acknowledgements**

Idaho Department of Fish and Game funded and conducted the fieldwork for this project. A phenomenal group of people, including Paul Atwood, David Dressel, Eric Freeman, Cheryl Hone, Mark Hurley, Zach Lockyer, Shane Roberts, Nathan Stohosky, Jen Struthers, Jamie Utz, and three years of field crews, contributed time to this project. It would not have been possible without their help.

My committee provided invaluable guidance throughout this project. Thank you for giving me so many extra chances after I earned the nickname you had for me. Dr. Hugh Robinson, you pushed back against my cynicism and tempered my enthusiasm with your own cynicism to keep me grounded. Having you two floors away whenever I had questions, hit roadblocks, or just wanted to talk to a friend instead of work has been a privilege. I promise to have the notes from our first meeting on the wall when it is your turn to visit. Dr. Mike Mitchell, thank you for showing me it is okay to struggle. You helped me get my head back above water, and your kind words have inflated my head to make sure it stays there. Whenever you read this, you probably owe me a beer. Dr. Paul Lukacs, thank you for reminding me that my work was worthwhile; your enthusiasm was contagious. Dr. Dave Ausband, thank you for organizing the field work and data collection. Your patience as I stumbled through data sharing and organization has taught me a lot about collaborating.

Kathy Zeller reanalyzed a data set to provide the movement speed estimate in Chapter 2. Thank you for than information and for being so generous with your time.

Millions of pictures were scored for this project which would not have been possible without the hard work of Paige Childers, Dominic Noce, Markis Scheu-Reyes, and Morgan Wilson.

The Wildlife Biology Program and Montana Cooperative Wildlife Research Unit supported me throughout this project. Thank you, Tina Anderson, Emmy Graybeal, and Debora Simmons, for patiently re-teaching me how to fill out paperwork each time.

I also want to thank the community I found in and around the Wildlife Biology Program. The Mitchell Lab: Kristin Barker, Sarah Bassing, Jesse Devoe, Kari Eneas, Shannon Forshee, James Goerz, Teagan Hayes, Ally Keever, Brandon Kittson, Collin Peterson, Sarah Sells, and Alex Welander; the Lukacs Lab: Colter Chitwood, Gus Geldersma, Jenny Helm, Charlie Henderson, Michelle Kissling, Jess Krohner, Molly McDevitt, Anna Moeller, Josh Nowak, Kaitlyn Strickfaden; and my extra-lab friends: Stephanie Berry, Shea Coons, Jessie Golding, Forrest Henderson, Mitch Johnson, Ellen Pero, and Kayla Ruth all deserve recognition. You taught me how to be a better scientist and human. I hope I can pass on your influences, both the good and the fun.

Finally, my community outside of wildlife helped me recover and maintain my emotional and mental health during this project. To my parents, Anna and Peter, does this count as “work”? To my brother, Stephen, I had to make sure we were at least tied. To Evelyn, you do more than you think. And to Sean, I appreciate you half as well as you deserve.

## **Chapter 1**

### **Introduction**

Wildlife biology relies on estimates of animal abundance for addressing ecological questions and informing management decisions. Many methods exist to estimate abundance (Schwarz and Seber 1999), but all rely on observing individuals in the population. Cryptic species that live at low-densities are difficult to observe, limiting the tools available for estimating abundance. Trapping and genetic sampling have been used, but both methods have drawbacks. Physically capturing individuals is invasive and requires intensive effort that can become expensive. Non-invasive genetic sampling eliminates the need to capture individuals, but analyzing the samples has high lab costs and can take considerable time, creating a lag between data collection and application (Lukacs and Burnham 2005, Waits and Paetkau 2005).

Despite requiring a large initial investment in equipment and high image analysis effort, remote cameras can be a useful tool for observing cryptic species that live at low densities. The first abundance estimates with remote cameras used capture-recapture methods and required species with naturally occurring marks that make individuals uniquely identifiable (Karanth 1995, Karanth and Nichols 1998). Mark-resight (Arnason et al. 1991) and spatial mark-resight (Sollmann et al. 2013b, 2013a) models relax the uniquely identifiable requirement by allowing estimation of partially marked populations and populations with marked but not identifiable individuals. However, mark-resight models still require that some portion of the population be distinguishable, which is not the case for many populations of interest.

There are currently two broad approaches to estimate abundance of unmarked populations with remote cameras: one treats the photographic data as spatially and temporally replicated counts, and a second models the encounter process between animals and the camera

view sheds. Methods that treat camera data as repeated counts, including N-mixture models (Royle 2004), spatial count models (Chandler and Royle 2013), and instantaneous sampling (Moeller et al. 2018), are inefficient for populations at low densities. However, the N-mixture and spatial count models also have assumptions that can be difficult to meet and test in field settings without auxiliary data, such as movement data from the population (Chandler and Royle 2013, Keever et al. 2017). The random encounter model (Rowcliffe et al. 2008) and space and time-to-event models (Moeller et al. 2018) estimate abundance from the encounter rate of animals moving with respect to randomly or systematically placed cameras. Estimating abundance by modelling the encounter process between animals and cameras has shown promise for low-density species (Cusack et al. 2015) but has not been widely adopted.

The time-to-event model (Moeller et al. 2018) estimates abundance by quantifying the relationship between density and encounter rate. Time-to-event analysis, also called survival analysis and failure time analysis, uses repeated measurements of the amount of time that elapses before an event of interest occurs to estimate the rate of that event. When we estimate density from camera traps, the event of interest is an animal appearing in the view shed, or a detection, and the rate of interest is density, or the number of animals per view shed. To estimate density from repeated measures of the time until an animal appears in a view shed, the model makes four assumptions.

First, the time-to-event models assumes that spatial counts of animals, or the number of animals in a given area, are Poisson-distributed at the scale of a camera view shed. Ecologists commonly use the Poisson distribution to model count data (Thomas 1949). The counts of animals in a given area will be Poisson-distributed if individuals are equally likely to be in any section of a landscape and the location of one individual does not affect the location of other



individuals. In field sampling, this assumption could be violated by animals grouping together, potentially due to clumped resources or social behavior, or by animals avoiding each other, potentially due to territoriality. Violating the Poisson-distributed assumption should bias the estimate low for aggregated populations and high for evenly dispersed populations, however, the model may be robust to some degree of aggregation or dispersion. Camera view sheds sample a small area relative to animal densities, so, even when animals aggregate around a resource, most counts of animals in the view shed will be 1 or 0 individuals, as expected under a Poisson distribution at low densities.

Second, the model assumes that animals move randomly with respect to the cameras. The model estimates the average density of the population from the rate that animals enter view sheds. Attempting to increase capture frequency by baiting cameras or by targeting roads, trails, or preferred habitat will bias the density estimate high if capture frequency is successfully increased. In practice, placing the cameras on the landscape randomly or systematically should meet the random movement assumption.

Next, the time-to-event model requires an accurate estimate of movement speed (including rest time) for the population. At constant density, encounter rate increases linearly with increasing animal movement speed, so any model that estimates density from encounter rate needs to account for movement speed (Carbone et al. 2001). In the time-to-event model, if movement speed increases, the observed time until an animal appears on camera will decrease, and the density estimate will be inflated.

Finally, the model assumes that the population is closed during sampling. Studies generally approximate closure by limiting sampling to a short period of time, but estimates of populations at low densities are more precise with the additional data from longer sampling

frames (Bischof et al. 2014, Dupont et al. 2019). In study designs that use an estimate of detection probability to estimate abundance, violating closure can bias the estimate of detection probability and subsequently abundance. The time-to-event model does not rely on an estimate of individual detection probability, so it handles lack of closure differently. The time-to-event model should estimate the mean density through time when density changes during a survey.

Most studies will fail to meet at least some of the assumptions of the model, therefore, before adopting these models more broadly, researchers need to understand the effects of violating assumptions on model performance. I used simulated walk models (Carbone et al. 2001, Codling et al. 2008) to test the effect of violating assumptions on the bias and precision of density estimates from the time-to-event model under five scenarios. In each scenario, I modified a simple random walk model to test the effect of violating one of the model assumptions. In the first scenario, I looked at the effect of estimating the movement speed of the population inaccurately by changing how far individuals move in the simulation. When movement speed was under-estimated, I expected density to be over-estimated, and vice versa. In the second scenario, I tested the effect of violating the closure assumption by removing individuals during the simulation. When the population was open, I expected the time-to-event model to estimate mean density through time. In the third scenario, I tested the effect of animals being more evenly distributed than predicted by a Poisson distribution by restricting individual movement to partially-overlapping areas representing territories. I did not expect the “territories” to have any effect on the time-to-event model, because, even with completely random movement, most cameras only have one animal in the view shed at a given time. The final two scenarios tested the effect of violating the Poisson assumption and the random movement assumption by simulating movement with respect to a randomly generated habitat with two camera placement strategies:

random placement and cameras placed to target the preferred habitat. For both camera placement methods in the habitat scenario, I applied two versions of the time-to-event model: the basic model and a second version that adjusts the density estimate for spatial variation in density using habitat covariates. In the randomly placed camera scenario, I expected both the basic model and the version adjusting for spatial variation in density to accurately estimate density. In the scenario with targeted camera placement, I expected the basic model to over-estimate density and the version adjusting for spatial variation in density to counteract the bias caused by targeted camera placement.

## Methods

### *Time-to-Event Model*

If the number of animals in camera view sheds is Poisson-distributed, the number of animals ( $N$ ) that pass through the camera view shed during a period of time is Poisson-distributed around density ( $\lambda$ ).

$$N \sim \text{Pois}(\lambda) \quad (\text{Equation 1})$$

In time-to-event analysis, the time that passes until a Poisson-distributed event occurs ( $TTE$ ) is exponentially distributed around the rate parameter ( $\lambda$ ), in this case density.

$$TTE \sim \text{Exp}(\lambda) \quad (\text{Equation 2})$$

Because the time until a Poisson distributed event occurs is exponentially distributed around density, we can estimate density with repeated measures of  $TTE$ .

Sampling for the time-to-event model requires definitions for two time intervals. First, the number of animals passing through the view shed during a time period ( $N$ ) depends on the length of the period. If the length of the period is equal to the amount of time the average animal

takes to pass through a view shed,  $N$  will be distributed around the mean number of animals per view shed, or density ( $\lambda$ ). Setting the length of the period requires an estimate of mean movement speed of the population (including rest time) and a measurement of the distance across the view shed. Second, sampling requires a defined occasion, or the amount of time spent observing the view shed waiting for an event to occur. If an event does not occur during the sampling occasion, it is recorded as a right censored event. Breaking the study into sampling occasions allows multiple measurements of  $TTE$  for each camera. Defining the length of occasions as some number of periods (e.g. five periods per occasion) allows  $TTE$  to be recorded as the number of periods until an event occurs (e.g. if an animal appears on camera during the first period,  $TTE$  is one for that occasion; if an animals appears during the fifth period,  $TTE$  is five).

The time-to-event model accommodates spatial variation in density. The basic application of the model estimates a single mean density across the sampled landscape, however, repeated measures of  $TTE$  for each camera allow for a density estimate at each camera. The variation in density between cameras can be modelled as the result of spatial covariates with a generalized linear model,

$$\log(\lambda_i) = \beta_0 + [\beta X_i] \quad (\text{Equation 3})$$

where  $\lambda_i$  is the estimated density at camera  $i$  and  $[\beta X_i]$  represents spatial covariates of camera  $i$  and their coefficients. With estimates for the effects of spatial covariates, the density of animals across the study area,  $\bar{\lambda}$ , can be estimated using

$$\log(\bar{\lambda}) = \beta_0 + [\beta \bar{X}] \quad (\text{Equation 4})$$

where  $\bar{X}$  represents the mean value, across the entire study area, for the spatial covariates.

*Walk Models – Control*

To test the effect of violating assumptions in each scenario, I compared them to a control simulation. In the control simulation, 16 individuals moved randomly within a 100x100-unit square. Distance measurements do not have a defined unit in the simulation, so they can be thought of at any scale. I divided the square into 36 cells with one detector, representing a camera trap with perfect detection, placed randomly in each cell. Detectors recorded an individual if the individual passed within a radius of  $\pi/4$  units of a detector during a given step. I used a radius of  $\pi/4$  units for the detectors so that the average path across the circular detection zone was 1 unit long. Each individual took 1000, 1-unit steps during the simulation, with turns at random angles every 5 steps. When a movement path would leave the 100 by 100 square, I flipped the x or y-axis portion of that step and subsequent steps until the next turn to keep the individual in bounds. I defined periods as one step in the simulation, so recording the step at which a detection occurred also recorded *TTE*. I set occasion length equal to five periods. I ran each simulation for 500 iterations.

### *Walk Models – Speed*

For the simulation testing the effect of incorrectly estimating animal movement speed, I modified the step length while keeping the other variables constant. Modifying step length and keeping the other variables constant simulates incorrectly estimating movement speed. If step length equals 0.5, rather than 1, it will take individuals two steps to cross a detection zone. If step length equals 2, it will only take half a step to cross a detection zone. I used a range of 15 different step lengths (0.5, 0.6, 0.7 ... 1.4, 1.5) to capture the trend in incorrectly estimating movement speed.

### *Walk Models – Open Population*

To test the effect of violating the closure assumption, I simulated the population decreasing during the survey. The time-to-event model should estimate the mean abundance through time, so I set the starting population and removal times to keep the mean abundance through time equal to the control population. I started with 20 individuals and censored individuals randomly throughout the survey until only 12 individuals remained. I censored individuals at random time steps, but, in each run, individuals were removed to ensure that the average population, weighted by time, was 16 individuals, the same as the control simulation.

### *Walk Models – Territoriality*

To test the effect of animals being more evenly distributed than expected under the Poisson assumption, I simulated individuals moving in territories. I simulated simple territories by specifying the start location of each individual and restricting their movements in a radius around the start location. I arranged the 16 start locations in a grid, with the first individual starting at  $(x = 12.5; y = 12.5)$  and the last individual starting at  $(x = 87.5; y = 87.5)$ . The nearest neighbors for each individual started 25 units away on the x or y-axis. Individuals moved randomly within a radius of 12.5 units around their start location. When individuals left that radius, subsequent turn angles tended towards the individual's start location, with the strength of the effect increasing with distance. Those movement rules result in a circular area used by each individual with more time spent near the center of the "territory".

### *Walk Models – Habitat – Random Cameras*

For the two scenarios testing the effect of animals clustering more than expected under the Poisson assumption, I had individuals move preferentially toward high quality habitat on a simulated landscape. To generate the landscape, I drew random habitat quality scores from a normal distribution at two levels of hierarchy, 16 large cells each divided into 625 sub-cells. The first level of hierarchy divided the landscape into a 4 by 4 grid, with the mean habitat quality score for each of the 16 cells drawn from a standard normal distribution. The second level of hierarchy provided habitat values for each sub-cell drawn from a normal distribution centered on the mean value of the habitat quality score of the cell. The resulting landscape consists of 16 cells, each 25 by 25 sub-cells, with habitat quality scores that tend to be more similar within cells than between cells (Fig. 1).

I used a simplistic model of animal movement relative to habitat to simulate preference for higher habitat quality scores. For each new angle an individual selected, I averaged the habitat scores along eight potential paths, the paths that go in a cardinal direction and the paths halfway between any two cardinal directions. I generated the actual turn angle from a circular distribution centered on the direction with the highest average habitat quality score. Randomly drawing the direction of travel results in individuals tending toward the best adjacent habitat with the variance allowing occasional movements away from the best habitat to prevent individuals from getting stuck in one part of the landscape (Fig. 1). I fit the basic time-to-event model in which mean density is estimated directly from the observed *TTE* (equation 2) and the model estimating density by adjusting for habitat with a generalized linear model (equations 3 and 4).

*Walk Models – Habitat – Targeted Cameras*

To test the effect of non-random movement with respect to the cameras, I placed cameras non-randomly with respect to the simulated landscape. The simulations of targeted camera placement use the same habitat generation and habitat preference rules as the habitat simulations with random camera placement. In all of the previous simulations, I placed one camera randomly in each of 36 sampling cells. In the targeted camera placement simulation, I assigned each camera to the sub-cell with the single highest habitat quality score in each sampling cell. This targeted sampling maximized detections, as might be the goal in capture-recapture or occupancy studies. However, for time-to-event studies, sampling to maximize detections will inflate the density estimate by lowering the observed TTE. Again, I estimated density twice for each run of the simulation, once without adjusting for habitat, and once adjusting for habitat with the generalized linear model (GLM).

### *Statistical Methods*

I used Bayesian methods to estimate abundance from each run of the simulations using Markov chain Monte Carlo (MCMC) implemented in JAGS (Plummer 2017) through R (R Core Team 2019) and the R2jags package (Su and Yajima 2015). I could not assess model fit for each run of the simulations individually, so I ran each model for a burn-in of 10,000 steps then updated the model in batches of 100,000 steps of 3 chains until the Gelman-Rubin convergence diagnostic ( $\hat{R}$ ) (Gelman and Rubin 1992) was less than 1.1. I discarded any simulations that failed to achieve an  $\hat{R}$  value less than 1.1 within 500,000 steps. The posterior distributions of the initial runs were symmetrical, so I recorded the mean of the posterior as the estimate of abundance and the standard deviation (SD) as a measure of precision to save computing memory during the simulation runs.



I examined the bias and the precision of the estimator for each simulation scenario. I used mean error (ME) to measure unscaled bias

$$ME = 1/n \sum_{j=1}^n (E_j - A) \quad (\text{Equation 5})$$

where  $n$  is the total number of runs of the simulations,  $E_j$  is the estimated abundance on the  $j^{\text{th}}$  run of the simulation, and  $A$  is the true abundance. ME is an unscaled measure of bias, so ME = 1 indicates that the model over-estimated by one individual on average and ME = -1 indicates that it under-estimated by one individual. I used SD of the estimated abundances from each scenario to examine the observed precision

$$SD = \sqrt{1/n \sum_{j=1}^n ((E_j - \bar{E})^2)} \quad (\text{Equation 6})$$

where  $n$  is the total number of runs of the simulations,  $E_j$  is the estimated abundance on the  $j^{\text{th}}$  run of the simulation, and  $\bar{E}$  is the mean of the estimates of abundance. Precision and SD are inversely related, so a lower SD indicates more precision. I compared the observed SD of the estimates of abundance to the mean of the SDs from the model's posterior distributions to check the accuracy of the precision estimates from the time-to-event model.

## Results

### *Control*

In the control simulation, the time-to-event model estimated a mean of 15.24 (Table 1) animals, slightly below truth ( $N = 16$  individuals). The SD of the estimate was 1.95, and the average standard deviation of the posterior distributions was 1.48, meaning that the model over-estimated precision. Precision was over-estimated in all of the simulations.

### *Speed*

Incorrectly estimating speed had a linear effect on abundance estimates in the simulation (Fig. 2). At the low end of the tested speeds (step length = 0.5),  $\bar{x}$  abundance was 9.20 (SD = 2.16). At the high end of the tested speeds (step length = 2) the mean abundance estimate was 28.36 (SD = 2.29) (Table 1).

#### *Open Population*

In the simulation that tested the effect of violating closure by removing part of the population during the simulation, the time-to-event model estimated the mean abundance as 15.44 individuals (SD = 2.03) (Table 1). That resembles the control simulation (Fig. 3b) and the mean abundance of 15.44 individuals is close to the mean abundance through time in the open population simulation (16 individuals).

#### *Territoriality*

The results from the simulations that violated the Poisson assumption by restricting animals to “territories” resembled the control simulation (Fig. 3a). The estimated abundance from the territorial simulation was 15.35 individuals (SD = 2.09) (Table 1).

#### *Habitat – Random Cameras*

In the habitat simulations with randomly placed cameras, the estimates began to diverge from the control slightly but remained in the same general range (Fig. 3c). The model with no adjustment for spatial variation in density returned a mean estimate of 16.39 individuals (SD = 2.63), while the model using the GLM to adjust for habitat returned a mean estimate of 12.62 individuals (SD = 2.97) (Table 1).

#### *Habitat – Targeted Camera Placement*

In the habitat simulations with targeted camera placement designed to maximize detections, both the basic model and the model using a GLM to adjust for habitat failed to

accurately estimate abundance (Fig. 3d). The basic model over estimated abundance (mean  $N = 26.37$ ;  $SD = 3.35$ ) while the GLM adjusted model underestimated abundance (mean  $N = 10.18$ ;  $SD = 5.02$ ).

## **Discussion:**

These simulations showed that the time-to-event model is robust to many of the scenarios encountered in studies of wild populations that violate the model assumptions. Neither territoriality of a species, nor open populations bias the results of the model. When animals move non-randomly with respect to habitat, the model is unbiased as long as cameras are placed randomly. However, both targeting high quality habitat when placing cameras and incorrectly estimating movement speed bias the estimate of density.

In the control simulation using a simple random walk, the time-to-event model accurately estimated abundance. The mean of the estimates (15.24 individuals) was slightly below truth (16 individuals), but was still within a single standard deviation. Moeller et al. (2018) also found a small negative bias in the time-to-event model using random walk simulations. This similarity in bias may be due to similarities in our walk simulations. The time-to-event model also over-estimated precision, with the mean estimated standard deviation approximately half an individual smaller than the observed standard deviation of the estimates.

Incorrectly estimating speed caused a linear bias in the abundance estimate (Fig. 2) with over estimates of speed causing under estimation of abundance and vice versa, as expected. When speed is under estimated, detection periods are too long. Animals moving faster than the estimated speed encounter cameras during a greater portion of those detection periods, causing an over estimation of abundance. The potential bias caused by misestimating movement speed

means that the time-to-event model requires auxiliary data. Estimating movement speed with GPS (global positioning system) collar data from the population being sampled is the most reliable option, but, for well-studied species that do not show significant variation in movement speed between populations, data from previous studies could suffice. If movement data were unavailable or unreliable, the space-to-event model may be more applicable but will be less precise (Moeller et al. 2018).

Neither territoriality nor closure violations affected the time-to-event abundance estimates (Figs. 3a and 3b). The mean and standard deviations for the territoriality and open population simulations were similar to the control simulation (Table 1). The open population simulation shows that the time-to-event model handles closure differently than capture-recapture models. Capture-recapture methods rely on estimating the probability of detecting individuals to estimate abundance ( $N$ ) with  $\hat{N} = \frac{C}{\hat{p}}$  where  $C$  is the observed count of animals and  $\hat{p}$  is the estimated detection probability (Nichols 1992). When individuals are present and available to be detected during one portion of a survey, but not another, detection probability is under-estimated and abundance is over-estimated, approximating the total number of animals that were in the study area during some portion of the survey. In contrast, the time-to-event model estimates the mean density through time. This means that lack of closure does not bias the estimate in the same way it does in capture-recapture studies, potentially allowing sampling over a longer time frame.

When animals are moving non-randomly with respect to habitat, the time-to-event model requires cameras be placed to sample the habitat randomly. In the habitat simulations with randomly placed cameras, both the base model and the model adjusting for habitat with a GLM returned estimates comparable to the control simulation (Fig. 3c) with the estimate from the base model slightly greater than the control and the estimate from the GLM adjusted model slightly

below the control. In the habitat simulations, both versions of the model are less precise than in the simple random walk simulation, and, in the base model, the precision was more inflated than in the control. Accounting for the effect of habitat on density with a GLM helps estimate the precision of the time-to-event model more accurately when animals move non-randomly with respect to habitat.

Non-random sampling biases estimators (Fisher 1925). In the time-to-event model, targeting landscape features to maximize detections will be the most common form of non-random sampling. In the patchy habitat simulations with targeted camera placement, the base time-to-event model greatly over estimated abundance (26 vs 16), and the time-to-event model with a GLM adjusting for habitat greatly underestimated abundance (10 vs 16). The under estimation of the GLM adjusted model may be caused by a non-linear effect of habitat. With the targeted camera placement, lower quality habitats were not sampled. If the relationship between density and habitat quality was different at the high and low ends of the habitat values, extrapolating to the un-sampled range of habitat values would fail. Further work should explore alternative sampling strategies that might provide unbiased estimates while still improving detection rates, such as targeting the best habitat with a portion of the cameras while placing the rest of the cameras randomly to sample the full range of habitat quality. However, monitoring a random sample of habitat by deploying cameras at randomly or systematically generated points, rather than sampling to maximize detections, remains the most reliable sampling technique for minimizing bias. Data from surveys with camera placement that was not designed to randomly sample the landscape are unlikely to provide unbiased estimates from the time-to-event model.

**Figures:**

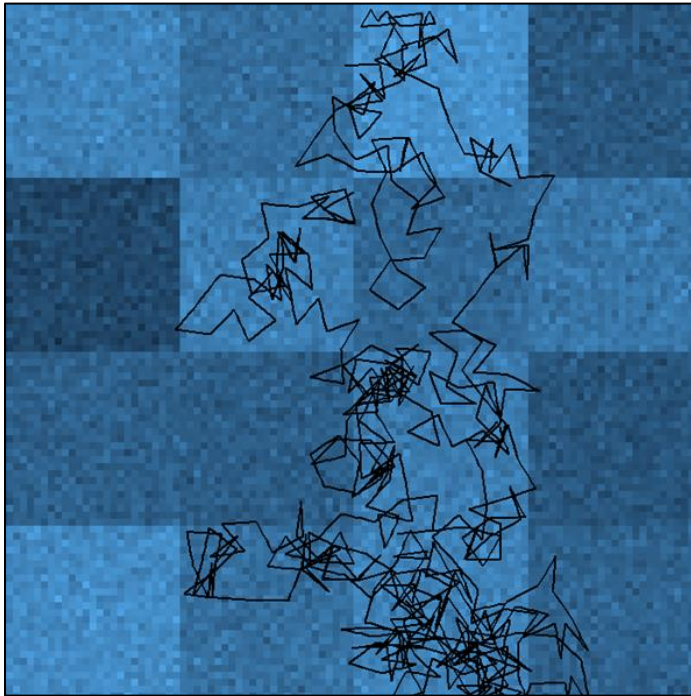


Figure 1: One animal path on a simulated landscape. Light colors represent preferred habitat. The animal tends toward preferred habitat and avoids less preferred habitat, resulting in clustered movement.

Simulation	Mean Estimate	SD of Estimates	Mean SD	Mean Error
Control	15.244	1.953	1.480	-0.756
Speed = 0.5	9.198	2.156	1.225	-6.802
Speed = 2	28.359	2.285	2.166	12.359
Open Population	15.437	2.027	1.490	-0.563
Territoriality	15.349	2.092	1.487	-0.651
Habitat – Random – Base	16.391	2.629	1.530	0.391
Habitat – Random – GLM	12.620	2.966	2.485	-3.380
Habitat – Targeted – Base	26.370	3.349	1.953	10.370
Habitat – Targeted – GLM	10.181	5.024	3.803	-5.819

Table 1: Summarized results from the walk simulations. Mean estimate is the mean of the reported abundance estimates from each iteration of the simulation. SD of estimates is the standard deviation of those means. Mean SD is the mean of the standard deviation from the posterior distributions. Mean error is a measure of the distance from truth of the estimates.

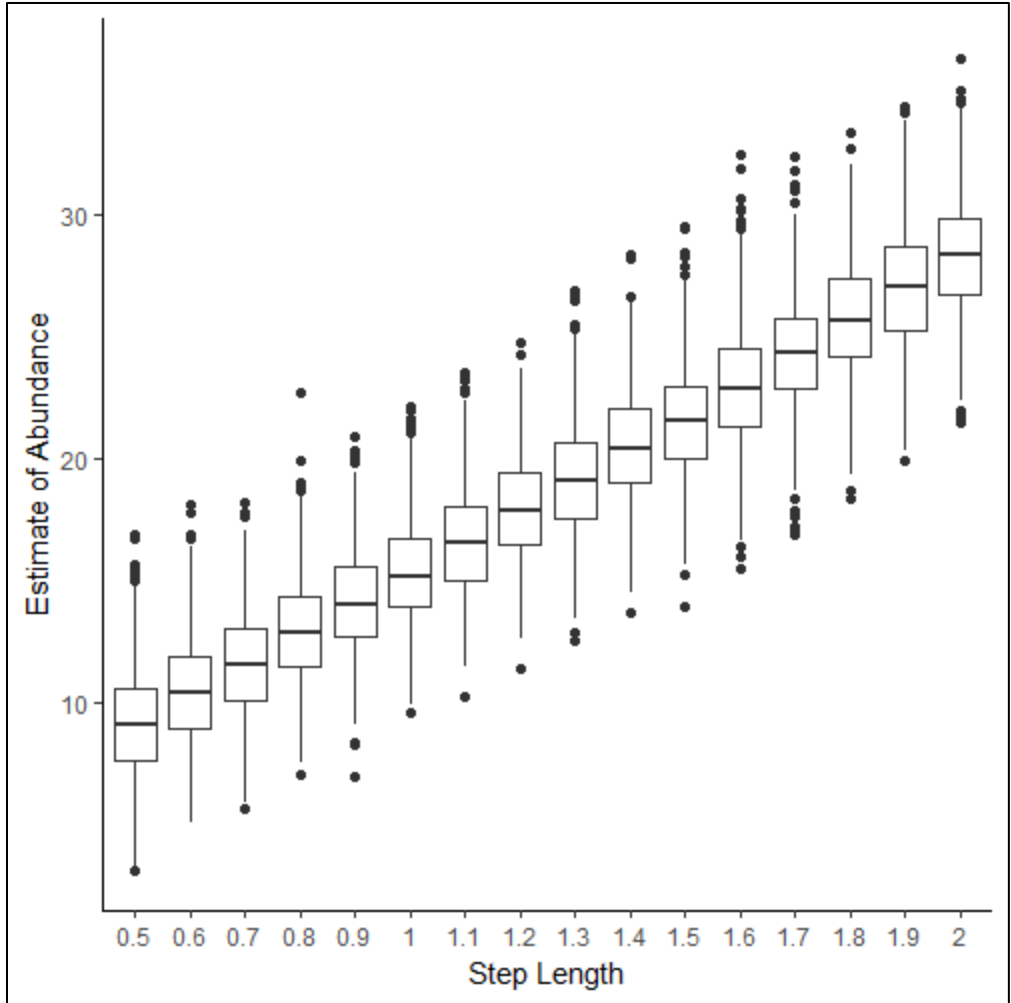


Figure 2: Box plots of mean abundance estimate by step length from the speed simulations. Each step length was simulated 1000 times.

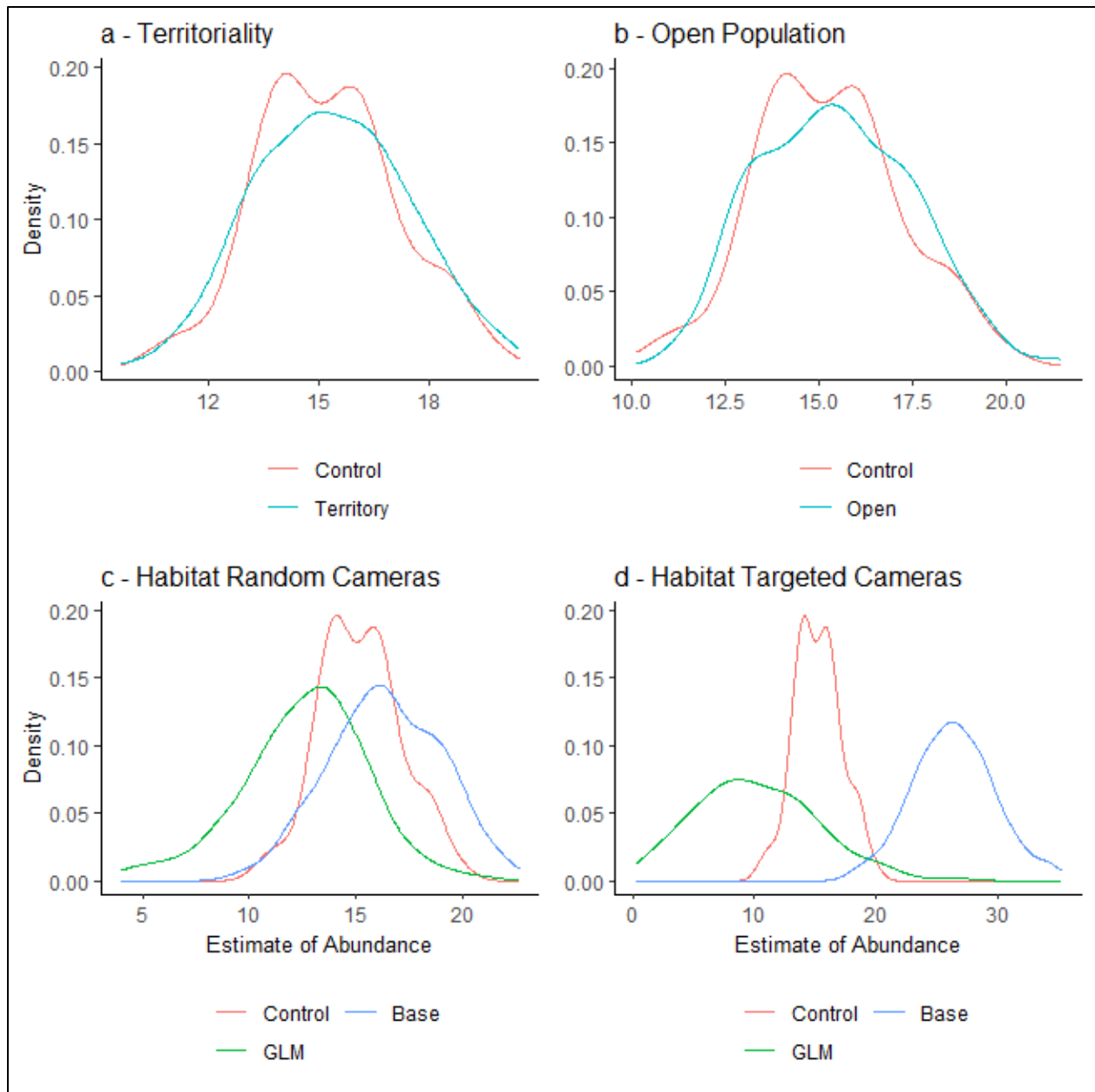


Figure 3: Trace plots of the histograms of mean abundance from (a) the territory simulation, (b) the open population simulation, (c) the habitat with randomly placed cameras simulations, and (d) the habitat with targeted cameras simulations. The results from the control simulation are plotted for comparison in all graphs. In c and d, the GLM line is the model using habitat values to adjust the abundance estimate and the Base line is the basic time-to-event model ignoring the habitat values.



## Literature Cited:

- Arnason, A. N., C. J. Schwarz, and J. M. Gerrard. 1991. Estimating Closed Population Size and Number of Marked Animals from Sighting Data. *The Journal of Wildlife Management* 55:716–730.
- Bischof, R., S. Hameed, H. Ali, M. Kabir, M. Younas, K. A. Shah, J. U. Din, and M. A. Nawaz. 2014. Using time-to-event analysis to complement hierarchical methods when assessing determinants of photographic detectability during camera trapping. *Methods in Ecology and Evolution* 5:44–53.
- Carbone, C., S. Christie, K. Conforti, T. Coulson, N. Franklin, J. R. Ginsberg, M. Griffiths, J. Holden, K. Kawanishi, M. Kinnaird, R. Laidlaw, A. Lynam, D. W. Macdonald, D. Martyr, C. McDougal, L. Nath, T. O'Brien, J. Seidensticker, D. J. L. Smith, M. Sunquist, R. Tilson, and W. N. Wan Shahrudin. 2001. The use of photographic rates to estimate densities of tigers and other cryptic mammals. *Animal Conservation* 4:75–79.
- Chandler, R. B., and J. A. Royle. 2013. Spatially explicit models for inference about density in unmarked or partially marked populations. *Annals of Applied Statistics* 7:936–954.
- Codling, E. A., M. J. Plank, and S. Benhamou. 2008. Random walk models in biology. *Journal of The Royal Society Interface* 5:813–834.
- Cusack, J. J., A. Swanson, T. Coulson, C. Packer, C. Carbone, A. J. Dickman, M. Kosmala, C. Lintott, and J. M. Rowcliffe. 2015. Applying a random encounter model to estimate lion density from camera traps in Serengeti National Park, Tanzania. *Journal of Wildlife Management* 79:1014–1021.
- Dupont, P., C. Milleret, O. Gimenez, and R. Bischof. 2019. Population closure and the bias-precision trade-off in spatial capture-recapture. *Methods in Ecology and Evolution* 10:661–

672.

- Fisher, R. A. 1925. Theory of statistical estimation. *Mathematical Proceedings of the Cambridge Philosophical Society* 22:700–725.
- Gelman, A., and D. B. Rubin. 1992. Inference from Iterative Simulation Using Multiple Sequences. *Statistical Science* 7:457–511.
- Karanth, K. U. 1995. Estimating tiger *Panthera tigris* populations from camera-trap data using capture-recapture models. *Biological Conservation* 71:333–338.
- Karanth, K. U., and J. D. Nichols. 1998. Estimation of Tiger Densities in India using photographic captures and recaptures. *Ecology* 79(8):2852–2862.
- Keever, A. C., C. P. McGowan, S. S. Ditchkoff, P. K. Acker, J. B. Grand, and C. H. Newbolt. 2017. Efficacy of N-mixture models for surveying and monitoring white-tailed deer populations. *Mammal Research* 62:413–422.
- Lukacs, P. M., and K. P. Burnham. 2005. Review of capture–recapture methods applicable to noninvasive genetic sampling. *Molecular Ecology* 14:3909–3919.
- Moeller, A. K., P. M. Lukacs, and J. S. Horne. 2018. Three novel methods to estimate abundance of unmarked animals using remote cameras. *Ecosphere* 9:e02331.
- Nichols, J. D. 1992. Capture-Recapture Models. *Bioscience* 42:94–102.
- Plummer, M. 2017. JAGS: Just Another Gibbs Sampler.
- Rowcliffe, J. M., J. Field, S. T. Turvey, and C. Carbone. 2008. Estimating animal density using camera traps without the need for individual recognition. *Journal of Applied Ecology* 45:1228–1236.
- Royle, J. A. 2004. N-Mixture Models for Estimating Population Size from Spatially Replicated Counts. *Biometrics* 60:108–115.

- Schwarz, C. J., and G. A. F. Seber. 1999. Estimating animal abundance: Review III. *Statistical Science* 14:427–456.
- Sollmann, R., B. Gardner, R. B. Chandler, D. B. Shindle, D. P. Onorato, J. A. Royle, and A. F. O’Connell. 2013a. Using multiple data sources provides density estimates for endangered Florida panther. *Journal of Applied Ecology* 50:961–968.
- Sollmann, R., B. Gardner, A. W. Parsons, J. J. Stocking, B. T. McClintock, T. R. Simons, K. H. Pollock, and A. F. O’Connell. 2013b. A spatial mark–resight model augmented with telemetry data. *Ecology* 94:553–559.
- Su, Y.-S., and M. Yajima. 2015. R2jags.
- Team, R. C. 2019. R: A Language and Environment for Statistical Computing. Vienna, Austria.
- Thomas, M. 1949. A Generalization of Poisson’s Binomial Limit For use in Ecology. *Biometrika* 36:18–25.
- Waits, L. P., and D. Paetkau. 2005. Noninvasive Genetic Sampling Tools for Wildlife Biologists: a Review of Applications and Recommendations for Accurate Data Collection. *Journal of Wildlife Management* 69:1419–1433.

## Chapter 2

### Introduction

Camera trapping is a common method for monitoring elusive species and species that live at low densities (O’Connell et al. 2011). When individuals in a population can be uniquely identified from photographs, camera trap data can be used to estimate abundance through capture-recapture and spatial capture-recapture (SCR) (Karanth 1995, Karanth and Nichols 1998, Royle et al. 2009). However, most species do not have uniquely identifiable individuals, so estimating abundance requires methods for unmarked populations. Quantifying the relationship between photographic rate and density (Carbone et al. 2001, Rowcliffe et al. 2008, Moeller et al. 2018) can be effective at estimating the abundance of elusive species that live at low densities and do not have unique marks (Cusack et al. 2015), but as yet none of these methods has been widely adopted.

The time-to-event and space-to-event models use time-to-event analysis to estimate density from the encounter rate between animals and cameras (Moeller et al. 2018). At higher densities, encounter rate is higher and the time between animals appearing on camera is shorter. The time-to-event model uses repeated measures of the time until an animal appears on camera and an estimate of animal movement speed to estimate density using

$$TTE \sim \text{Exp}(\lambda) \quad (\text{Equation 1})$$

where  $\lambda$  is density in animals per view shed and  $TTE$  is the observed distribution of the number of periods until an animal appears on camera. A period is defined as the time an animal moving at the mean movement rate of the population (including rest time) would spend in a view shed. If an animal appears during the first period,  $TTE$  is 1; if an animal does not appear until the third period,  $TTE$  is 3. For  $\lambda$ , the number of animals per view shed, to reflect the density of animals in

the study area, cameras must be placed randomly with respect to animal movement. The space-to-event model functions similarly but measures the amount of space sampled until an animal appears on camera at a point in time rather than measuring the amount of time until an animal appears at a given point in space. The space-to-event model estimates density using

$$STE \sim \text{Exp}(\lambda) \quad (\text{Equation 2})$$

where *STE* is the number of camera view sheds randomly sampled at a point in time before an animal is observed. The space-to-event model still requires cameras be placed randomly with respect to animal movement, but by sampling across cameras at a given time and allowing the animals to move between temporal samples, the space-to-event model eliminates the need for an estimate of animal movement speed.

Evaluating the efficacy of a new abundance estimator requires a point of comparison. Ideally, estimates are compared to truth by surveying a population of known size (Rowcliffe et al. 2008). However, populations of known size are not always available and often represent idealized conditions. When populations of known size are not available, estimates from the new method can be compared to reasonable expectations based on prior knowledge (Karanth 1995) or to estimates of the same population using accepted methods (Efford 2004).

Cougars (*Puma concolor*) are a challenging species to monitor because they are elusive, naturally unmarked, and live at low densities. Historically cougar populations were quantified using a census technique in which researchers attempted to collar or mark all resident animals in a study area (Hornocker 1969, Seidensticker et al. 1973). More recently cougar populations have been quantified using genetic SCR (Brochers and Efford 2008, Royle and Young 2008, Gardner et al. 2010) from surveys using unstructured spatial sampling to estimate cougar abundance (Russell et al. 2012, Proffitt et al. 2015) which requires high effort or auxiliary data (i.e. collar

data) (Paterson et al. 2019). The intensive effort required for both census attempts and genetic SCR techniques reduces their utility for broad scale monitoring. The time and space-to-event models can be applied to any sized study area and could be used to monitor multiple species from a single survey. However, estimating density from the time and space-to-event models requires deploying enough cameras for animals to encounter randomly placed cameras, potentially limiting its utility for species that live at low densities. I compared estimates of cougar abundance obtained using the time and space-to-event models to concurrent estimates based on genetic SCR at two field sites across multiple years.

## **Methods**

### Field sites

I sampled two study areas in Idaho, USA (Fig. 1) over 3 winters. Both study areas were classified as ungulate winter range by Idaho Fish and Game (IDFG). The first study area was located in Boise National Forest in central Idaho along the Middle and South forks of the Payette River. Elevation ranges from 850 meters to 2460 meters. The area receives 65.6 cm of annual precipitation, concentrated in the winter. Average winter snow cover (November to March) is 30.5 cm at 1200 meters. Average winter temperature is -1.7 °C, and average summer temperature (April to October) is 12.6 °C. The predominant vegetation type is mixed conifer forest. The dominant prey species are elk and mule deer (*Odocoileus hemionus*), and other large carnivores present are wolves (*Canis lupus*), black bears (*Ursus americanus*), and coyotes (*C. latrans*).

The second study area was in southeast Idaho along the western front of the Bear River Range. Elevation ranges from 400 meters to 2700 meters. The area receives 32.0 cm of annual precipitation with a spike in the spring and lull in the summer. The average winter temperature is

-1.2 °C and average summer temperature is 14.5 °C. At higher elevations, mixed coniferous forest is dominant, at lower elevations, sage brush steppe and juniper is dominant. The western edge of the study area extends into the cache valley which is dominated by agricultural fields. The dominant prey species is mule deer, and black bears and coyotes make up the rest of the large carnivore community, wolves are absent.

At both field sites, a grid of 10 km<sup>2</sup> cells was overlaid on ungulate winter range (Fig.2). In the Central Idaho site, the grid was defined using elk winter range. In the SE Idaho site, it was defined using a combination of elk and mule deer winter range. We used the same grid for the camera and genetic sampling. The Central Idaho site was surveyed during the winters of 2016-2017, 2017-2018, and 2018-2019. The SE Idaho site was surveyed in 2017-2018 and 2018-2019.

#### Camera Sampling

Camera trapping grids were established, set-up and maintained by IDFG staff. Two to three potential camera sites were identified for each cell based on riparian areas and predicted cougar travel corridors within the ungulate winter range (Blake and Gese 2016). Field crews selected one camera site to deploy a camera at in each cell based on ease of access. At the site, cameras were placed approximately 3 meters high in trees and pointed down on roads or game trails whenever possible. The width of each view shed was measured as the distance along the trail through which the camera triggered during walk tests. Due to the elevated camera placement, the width and height of the view shed appeared approximately equal, so I calculated the view shed area as:  $area = width^2$ . Cameras were deployed in September and October of each year and retrieved in April and May of the following year. Only pictures from November 1 through March 31 were used to limit inference to density on winter range.

#### Genetic Sampling

Genetic samples were collected from backtracking, harvest, and biopsy darting using hounds to tree cougars between December and March of each winter (Russell et al. 2012, Beausoleil et al. 2016). The backtracking and biopsy darting crews used unstructured spatial sampling to search for cougar tracks (Russell et al. 2012, Proffitt et al. 2015). Once a track was found, crews either backtracked it to search for hair and scat or followed it using hounds to tree the cougar. Rather than assign a certain amount of effort to each cell, search could adapt to access, snow availability, and presence of cougar tracks. Distance searched was recorded for each cell using GPS (global positioning system) track logs and used to account for variable effort between cells. Biopsy darting was conducted during the first year of sampling in Central Idaho (2016 – 2017) but then restricted to SE Idaho in 2017-18 and 2018-19.

#### Space/Time-to-Event

I used a movement speed estimate of 8.9 km travelled per day (Zeller unpublished data) and the mean of the view shed widths (7 meters) to define the sampling period as approximately 1 minute. I defined an occasion for the time-to-event model as 500 periods. For each occasion, the number of periods that passed before a cougar appeared,  $TTE$ , was recorded at each camera. After 500 periods, the measured  $TTE$  was recorded as right censored and a new occasion started. Density was estimated with

$$TTE_{jk} \sim \text{Exp}(\lambda) \quad (\text{Equation 1})$$

where  $TTE_{jk}$  is the time until an event occurs at camera  $k$  on occasion  $j$ , and  $\lambda$  is density measured in cougars per view shed. For the final reported density,  $\lambda$  was converted to cougars per 100 km<sup>2</sup> using an estimate of 50 m<sup>2</sup> for view shed area. For the space to event model, density was estimated using

$$STE_i \sim \text{Exp}(\lambda) \quad (\text{Equation 2})$$



where  $\lambda$  is still density in cougars per view shed, and  $STE_i$  is the number of cameras sampled randomly at each time step,  $i$ , until a cougar is observed. Samples for the space-to-event model were taken every 5 minutes and cougars were included as detected if they appeared on camera within 30 seconds of each 5-minute time step. Data were recorded as right censored if a cougar did not appear on camera at time step  $i$ . For both models,  $\lambda$  was estimated using log-likelihood, and 95% confidence intervals were calculated as  $\hat{\lambda} \pm (SE \times 1.96)$ .

### Spatial Capture-Recapture

For the spatial capture recapture (SCR) density estimate, I assigned each observation to a hypothetical trap at the center of the cell the observation occurred in. I modelled the probability of observing individual  $i$  at trap  $j$ ,  $p_{ij}$ , as

$$p_{ij} = p_{0j} \times g_{ij} \quad (\text{Equation 3})$$

where  $p_{0j}$  is the probability of observing a cougar with a center of activity at the location of hypothetical trap  $j$ , and  $g_{ij}$  is the effect of distance between the activity center and trap location (Proffitt et al. 2015).  $g_{ij}$  is modeled as a half normal decay function with

$$g_{ij} = \exp\left(\frac{-d_{ij}}{2\sigma^2}\right) \quad (\text{Equation 4})$$

where  $d_{ij}$  is the distance between the activity center of animal  $i$  and trap  $j$ , and  $\sigma$  controls the magnitude of the effect (Gardner et al. 2010, Russell et al. 2012). I used two different models for  $p_{0j}$ , one where it is held constant, and one where it varies based on the amount of search effort in cell  $j$  according to the generalized linear model

$$\text{logit}(p_{0j}) = B_0 + B_1 \times \text{Effort}_j \quad (\text{Equation 3})$$

where  $\text{Effort}_j$  is the centered and scaled distance searched in cell  $j$  (Russell et al. 2012, Proffitt et al. 2015).

I fit the SCR model in a Bayesian framework using JAGS (Plummer 2017) implemented through R (R Core Team 2019) with the rjags (Plummer et al. 2019) package. I augmented the observed encounter histories with 1000 all-0 encounter histories. Each encounter history is assigned as belonging to a real or imaginary animal, and abundance is estimated as the number of real animals. I buffered the trapping grid by 10 km in every direction and used a random uniform distribution within that buffered zone as the prior for activity centers. I used a diffuse normal distribution for the priors on  $B_0$  and  $B_I$  and a diffuse half normal distribution from 0 to infinity as the prior for  $\sigma$ . I ran each model for 5,000 iterations in the adaptation phase, discarded the next 20,000 iterations as burn-in, and kept 75,000 iterations, thinned by 10, as the posterior distribution.

I evaluated goodness of fit for the SCR models using two Bayesian P-values (Gelman and Rubin 1992), one for the encounter process and one for the spatial point process (Russell et al. 2012, Proffitt et al. 2015). For the encounter process, I compared the discrepancy measures of the observed encounter rate and an encounter rate simulated from the posterior distribution using

$$D = \sum_{i=1}^N (\sqrt{n_i} - \sqrt{e_i})^2 \quad (\text{Equation 4})$$

where  $D$  is the discrepancy measure,  $N$  is the total number of individuals,  $n_i$  is encounter frequency (observed or simulated) of individual  $i$ , and  $e_i$  is the expected encounter frequency of individual  $i$  under the model. The Bayesian P-value for the encounter process is the proportion of steps in the MCMC where  $D(\text{observed})$  is greater than  $D(\text{simulated})$ . For the goodness of fit test for the spatial point process, I used

$$I = (G - 1) \times s^2 / \bar{n} \quad (\text{Equation 5})$$

where  $G$  is the number of grid cells,  $\bar{n}$  is the average number of activity centers per grid cell, and  $s$  is the variance of activity centers in each grid cell. To calculate the Bayesian P-value, I

compared  $I$  calculated from the posterior distribution and  $I$  calculated from simulations of spatial randomness. The P-value is the proportion of times that  $I(\text{posterior})$  is greater than  $I(\text{simulated})$ . For both Bayesian P-values, values near 0.5 indicate good fit, and values near 0 or 1 indicate poor fit.

## **Results**

### Cameras

Due to variable effort and camera failures, the number of cameras functional for some portion of each survey varied between sites and years (Table 1) from a high of 77 cameras functional for a portion of the Southeast ID 2018 survey, to a low of 64 cameras for the Central ID 2019 survey. The number of occasions during which a cougar was observed for the space-to-event and time-to-event analyses also varied between surveys (Table 1).

Estimates of density from the two camera based models varied between years in the Central ID site and between models for the 2019 survey of the Central ID site (Fig. 3). In 2017, density in the Central ID site was estimated at 5.64 (3.98-7.29) cougars per 100 km<sup>2</sup> by the time-to-event model and 5.80 (1.52-10.08) cougars per 100 km<sup>2</sup> by the space-to-event model (Table 2). In 2019 both estimates were notably higher and diverged from each other, with the time-to-event model estimating 10.82 (8.36-13.29) cougars per 100 km<sup>2</sup> and the space-event-model estimating 21.40 (13.18-29.62) cougars per 100 km<sup>2</sup>. Estimates of density in the Southeast ID site were more consistent. In 2018, the time-to-event and space-to-event models estimated 6.19 (4.53-7.49) and 6.51 (2.64-10.37) cougars per 100 km<sup>2</sup> respectively. The estimates of density remained similar in 2019 with the time-to-event and space to event models estimating 5.55 (3.87-7.23) and 7.32 (2.52-12.13) cougars per 100 km<sup>2</sup> respectively.

## DNA based SCR

The number of individuals detected in the genetic sampling and the recapture rate (the average number of detections per individual) varied across surveys and were generally lower in the Central ID site where biopsy darting was restricted to 2017. At the Central ID site we detected 21, 16, and 6 individuals with recapture rates of 1.19, 1, and 1 in 2017, 2018, and 2019 respectively. A recapture rate of 1 indicates that no individuals were detected multiple times. At the Southeast ID site, we detected 32 and 18 individuals with recapture rates of 1.38 and 1.22 in 2018 and 2019 respectively.

The low recapture rates at the Central ID site were insufficient to perform SCR, so density estimates from the genetic sampling are restricted to the Southeast ID site. Including effort per grid cell as affecting cell specific detection probabilities did not change the estimates of density within years, but there was some variation in the estimates between years (Fig. 3). The SCR model estimated 6.47 (3.35-12.15) cougars per 100 km<sup>2</sup> in the Southeast ID site in 2018, and 3.17 (1.55-7.31) cougars per 100 km<sup>2</sup> in 2019 (Table 2). The null model fit the data well for both the encounter process and point process in both years, but including effort as affecting detection probability reduces the model fit for the encounter process, despite the effort covariate appearing significant (Table 3).

## **Discussion**

The results show that the time-to-event and space-to-event models are promising tools for estimating the abundance of species that live at low densities, but non-random camera placements may have biased the estimates of density in this study. In the SE Idaho site, the estimates of density from the two models were consistent with each other, the SCR estimates,

and within the range of cougar density estimates found in the literature (Russell et al. 2012, Proffitt et al. 2015). The estimates of density from the Central Idaho site were less consistent, with variation between years and between models within the same year. Much of this variation was likely due to sampling design. Cameras were placed non-randomly to target winter habitat. If the use of winter habitat by cougars varied between years based on snowfall or other winter conditions, the encounter rate, and thus the estimates of density, should also vary. Non-random camera placement might explain the variable estimates between years, but it cannot explain the divergence of the time-to-event and space-to-event estimates in Central Idaho in 2019 (figure 3a). The divergence of the time-to-event and space-to-event models might be caused by random chance and low sample size. The space-to-event model only uses the subset of detections that happen at a point in time for each occasion. In this study, the space-to-event time sample lasted 1 minute, and was taken every 5 minutes. Effectively, each cougar detection had a 1 in 5 chance of being used in the space-to-event model. At low sample sizes, that random chance could have an outsized impact on the density estimate. This effect is reflected in the large confidence intervals of the space-to-event estimates and should be minimized as the number of cameras and animal density increase.

Sampling in this study was not ideal for the time and space-to-event models, which may have biased the density estimates. Unlike other camera arrays designed for occupancy or SCR analyses where cameras are placed to maximize detection probability, the time and space-to-event models assume that animal movements are random in relation to camera placement (i.e. cameras are randomly located, (see chapter 1). In this study, cameras were placed non-randomly at three scales. First, the study area was defined by winter range. Defining the study area as a portion of the landscape means that the density estimates are only applicable to that portion of

the landscape. Here, density on winter range was estimated, which is comparable to the SCR estimates and to literature estimates of cougar density (Hornocker 1969, Seidensticker et al. 1973, Russell et al. 2012, Proffitt et al. 2015). Sampling to estimate density on cougar winter range matches the goals of this study but could contribute to variation in density estimates. Within winter range, camera locations were selected based on predicted cougar movement corridors. Finally, at the selected locations, cameras were placed on roads and trails whenever available. Placing cameras along predicted movement paths should increase detection rates and bias density estimates high. The exact area sampled by each camera was also measured imprecisely, with only the view shed width measured in the field. Estimating the area sampled incorrectly will also bias the density estimates.

Despite the potential bias from non-random camera placement within the winter ranges, the estimates of density show that the time-to-event model can be effective for species that live at low densities. The time and space-to-event models estimate the density of animals in camera view sheds, meaning that the view sheds must represent a random sample of the landscape to provide unbiased estimates. Species that live at low densities can be challenging to monitor with random sampling due to low encounter rates. In this study, sampling to maximize detection rates may have biased the estimates higher than true cougar density. However, the results do show that the model functions at densities as low as those found here (i.e. approximately 6 individuals /100km<sup>2</sup>) and the associated low detection rates. At densities lower than those found here, as might be expected with a completely random sample of these study areas, increasing the number of cameras might be necessary to ensure detections, but the time-to-event model is effective with low detection rates.

Both estimators performed comparably to SCR. For the surveys in which SCR estimated density, the time-to-event estimate was more precise, and the space-to-event estimate, which does not require any movement data, showed comparable precision to the SCR estimate. Both SCR and the camera-based estimators showed variation in the estimates for the same site between years and both performed poorly with sparse data. In some situations, the failure of the SCR model to estimate density might be preferable to the highly variable estimate returned by the space-to-event model when data are sparse, but in general, the space and time-to-event models appear to more reliably return an estimate of density than SCR when species are difficult to detect. SCR and capture-recapture methods more broadly rely on capturing the same individual multiple times, which can be difficult when capture probability is low. The individuals never detected do not contribute to the model. In contrast, the occasions with no animal detected are almost as informative to the time and space-to-event models as the occasions with an animal detected. Occasions without detections are expected when surveying a population at low density. The estimate of density from the space and time-to-event models depends as much on the ratio of occasions with detections to occasions without detections as it does on the observations (non-right censored occasions) of the time or space until an event occurs.

The time and space-to-event models also scale well compared to capture-recapture methods. Because SCR relies on capturing the same individual in multiple locations, it performs best when effort is concentrated in a small area. To survey a larger area, total effort has to increase to keep the effort per unit area, and thus the probability of recaptures, consistent. The time and space-to-event models do not rely on recapturing the same individual; they only use the encounter frequency of the study species across the entire study area. That means a survey using

100 cameras would be as effective at estimating density in a large study area as it would in a small study area.

Camera based estimators that scale to any size study area and effectively estimate the density of unmarked species could help address many of the issues with monitoring species such as cougars and make multi-species monitoring more feasible. Rare species and species that live at low densities typically require targeted effort to observe during surveys, perhaps limiting the utility of a survey for sympatric species. The space and time-to-event models rely on a random sample of the study area but can still effectively estimate the density of species living at low densities. A random sample of the study area will be random for every species, not just the target species, so monitoring multiple species would only be reliant on all target species being able to be detected by the same camera setup.

These models are an effective tool for monitoring the abundance of unmarked populations. Combining the efficiency of observing animals through remote cameras with the time-to-event approach allows the estimation of low-density populations without the need for individual identification. The methods are general enough to apply to many different species, with the low-density species tested here representing a difficult case. In this difficult case, biased camera sampling resulted in performance comparable to existing, intensive efforts. With randomly placed cameras and sufficient effort, these methods should provide reliable estimates of low-density populations, making them a viable option for monitoring a diverse array of species.

### **Management Implications**

The time-to-event and space-to-event models are effective tools for estimating the abundance of unmarked populations. Even for species at low densities, and thus low encounter



rates, when cameras are placed randomly, the models perform well given enough cameras, in this case approximately 10,500 trap days. Estimating the abundance of low-density, difficult to detect species using camera surveys, rather than intensive ground surveys or capture-recapture efforts, could make abundance estimates for those species more feasible and cheaper to obtain. With relatively efficient methods, point estimates of abundance could be used to inform management decisions more often or be obtained more frequently to inform existing integrated population models (IPMs) or management plans such as that currently employed by Montana Fish Wildlife and Parks (Montana Fish Wildlife and Parks 2019).

**Figures:**

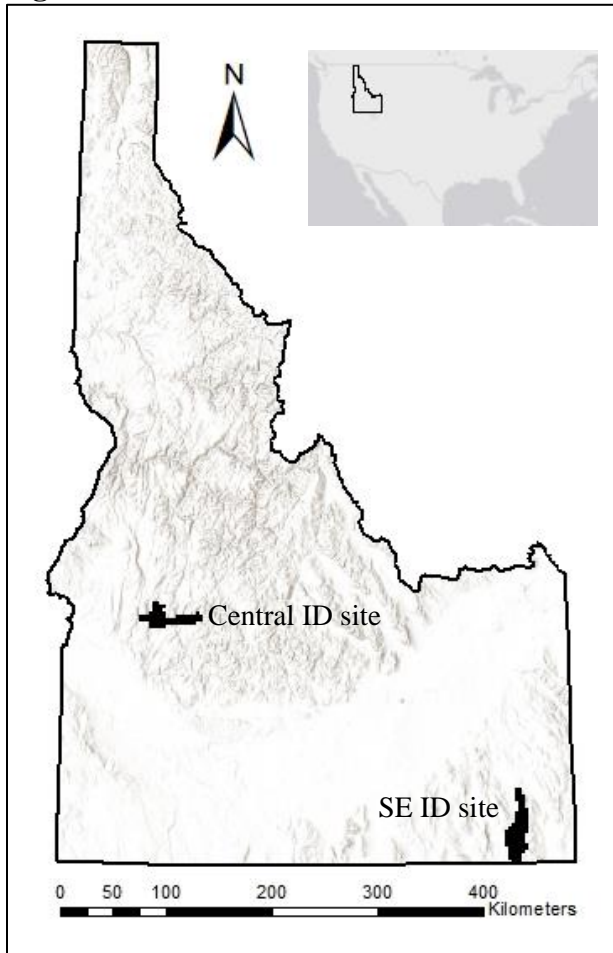


Figure 1: Shaded relief map of Idaho, USA with the Central and Southeastern sites in black. (Esri World Hillshade Base Map)

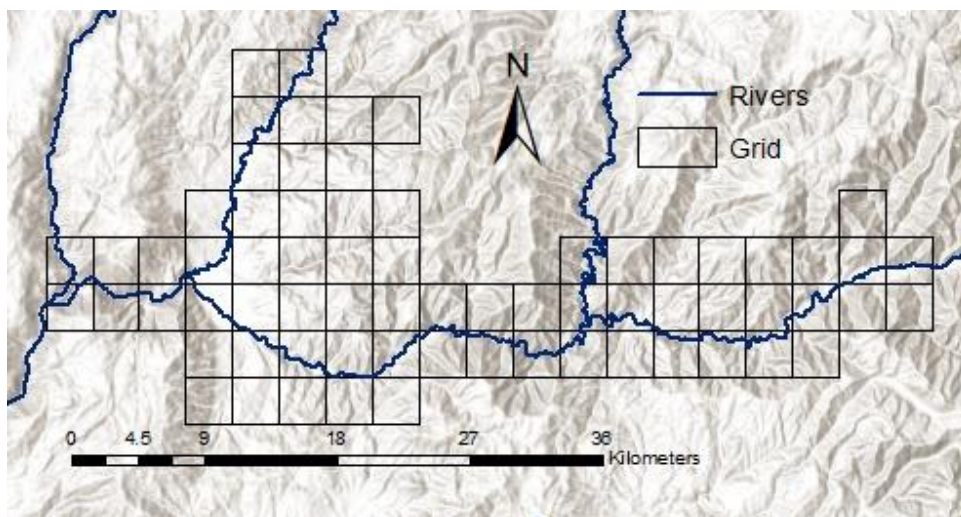


Figure 2: Map of the Central Idaho site showing local relief. Each grid cell is 10 km<sup>2</sup>. The extent of the study area was defined by predicted ungulate winter range. (Esri World Hillshade Base Map)

Site	Year	Cameras	TTE	STE
Central ID	2017	70	45	7
Central ID	2018	67	81	17
Central ID	2019	64	74	26
Southeast ID	2018	77	53	11
Southeast ID	2019	71	40	9

Table 1: The variation in camera effort between surveys. Cameras represents the number of cameras that were functional for at least a portion of the survey. TTE and STE are the number of occasions that were not right censored (a cougar appeared on camera) for the time-to-event and space-to-event analyses respectively.

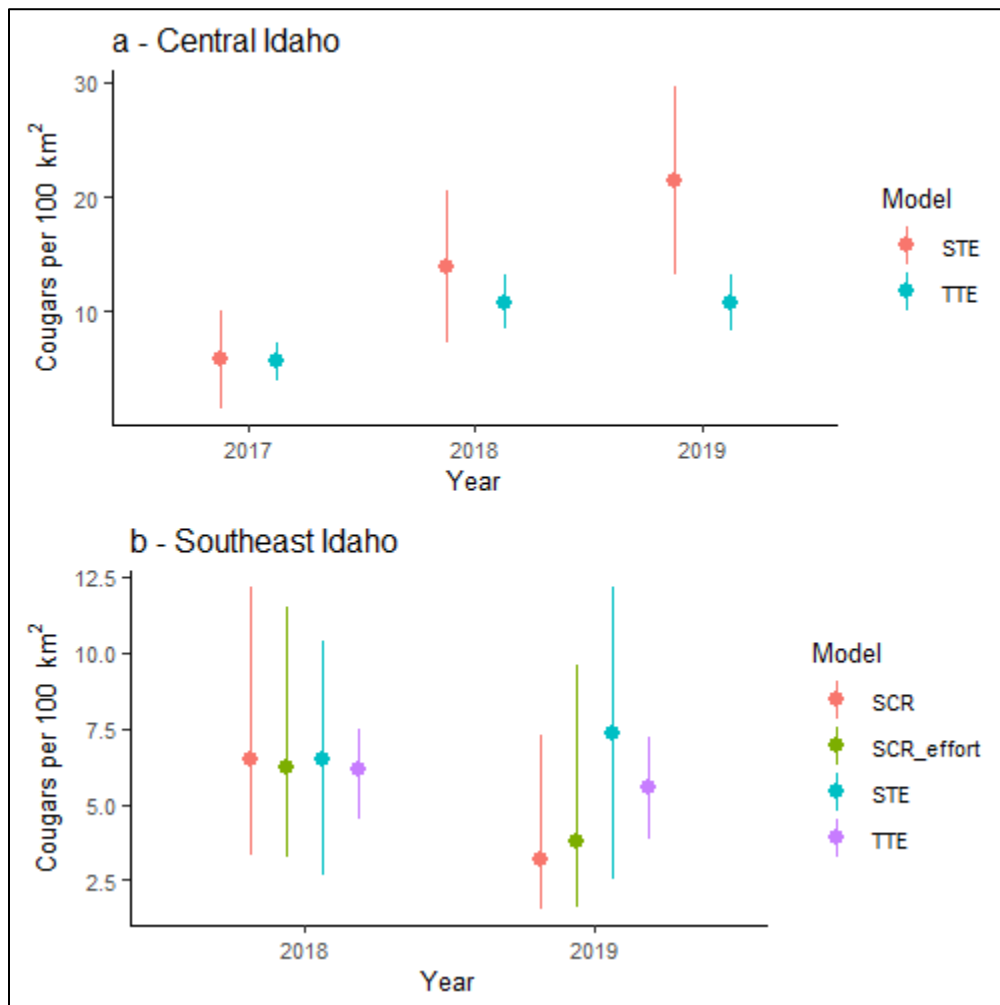


Figure 3: (a) Estimates of density and 95% CIs from the space-to-event and time-to-event models from the three surveys of the Central ID site. Insufficient recaptures prevented SCR estimates from the Central ID site. (b) Density estimates from the space-to-event, time-to-event, and two SCR models from the two surveys in the Southeast ID site. Intervals shown are 95% confidence intervals for the space and time-to-event models and 95% credible intervals for the SCR models.

Location	Year	Model	Mean	LCI	UCI
Central	2017	TTE	5.64	3.98	7.29
Central	2017	STE	5.80	1.52	10.08
Central	2018	TTE	10.84	8.48	13.20
Central	2018	STE	13.97	7.33	20.62
Central	2019	TTE	10.82	8.36	13.29
Central	2019	STE	21.40	13.18	29.62
Southeast	2018	TTE	6.19	4.53	7.49
Southeast	2018	STE	6.51	2.64	10.37
Southeast	2018	SCR	6.47	3.35	12.15
Southeast	2018	SCR - effort	6.19	3.26	11.50
Southeast	2019	TTE	5.55	3.87	7.23
Southeast	2019	STE	7.32	2.52	12.13
Southeast	2019	SCR	3.17	1.55	7.31
Southeast	2019	SCR - effort	3.81	1.63	9.59

Table 2: Estimates of density from each site, survey, and model. Mean is the estimate of density in cougars per 100 km<sup>2</sup> for each survey from each model. LCI and UCI are bounds of 95% confidence intervals for time-to-event and space-to-event. For the SCR models, LCI and UCI are the limits of the 95% credible interval.

Year	Model	Density	$B_{Effort}$	Sigma	Encounter	Point Process
2018	$B_0$	6.47 (3.35 – 12.15)	NA	3.49 (2.36 – 5.63)	0.36	0.52
2018	$B_0 + B_1Effort$	6.19 (3.26 – 11.50)	0.50 (0.16 – 0.91)	3.50 (2.32 – 5.61)	1.00	0.55
2019	$B_0$	3.17 (1.55 – 7.31)	NA	1.67 (1.14 – 2.97)	0.53	0.28
2019	$B_0 + B_1Effort$	3.81 (1.63 – 9.59)	2.20 (-0.63 – 9.01)	1.73 (1.13 – 3.33)	1.00	0.29

Table 3: Summarizes the results from the SCR models for the two surveys of the Southeast ID field site. Model indicates whether search effort within cells was included as affecting cell specific detection probability. Density is the estimated number of cougars per 100 km<sup>2</sup>.  $B_{Effort}$  is the estimate of the effect of centered and scaled search effort on detection probability. Sigma estimates the effect of distance between individual activity centers and cells on detection probability. Encounter and point process are Bayesian p-values representing how well the data fit the model.

## Literature Cited

- Beausoleil, R. A., J. D. Clark, and B. T. Maletzke. 2016. A long-term evaluation of biopsy darts and DNA to estimate cougar density: An agency-citizen science collaboration. *Wildlife Society Bulletin* 40:583–592.
- Blake, L. W., and E. M. Gese. 2016. Resource selection by cougars: Influence of behavioral state and season. *Journal of Wildlife Management* 80:1205–1217.
- Brochers, D. L., and M. Efford. 2008. Spatially explicit maximum likelihood methods for capture-recapture studies. *Biometrics* 64:377–385.
- Carbone, C., S. Christie, K. Conforti, T. Coulson, N. Franklin, J. R. Ginsberg, M. Griffiths, J. Holden, K. Kawanishi, M. Kinnaird, R. Laidlaw, A. Lynam, D. W. Macdonald, D. Martyr, C. McDougal, L. Nath, T. O'Brien, J. Seidensticker, D. J. L. Smith, M. Sunquist, R. Tilson, and W. N. Wan Shahrudin. 2001. The use of photographic rates to estimate densities of tigers and other cryptic mammals. *Animal Conservation* 4:75–79.
- Cusack, J. J., A. Swanson, T. Coulson, C. Packer, C. Carbone, A. J. Dickman, M. Kosmala, C. Lintott, and J. M. Rowcliffe. 2015. Applying a random encounter model to estimate lion density from camera traps in Serengeti National Park, Tanzania. *Journal of Wildlife Management* 79:1014–1021.
- Efford, M. 2004. Density estimation in live-trapping studies. *Oikos* 106:598–610.
- Gardner, B., J. A. Royle, M. T. Wegan, R. E. Rainbolt, and P. D. Curtis. 2010. Estimating Black Bear Density Using DNA Data From Hair Snares. *Journal of Wildlife Management* 74:318–325.
- Gelman, A., and D. B. Rubin. 1992. Inference from Iterative Simulation Using Multiple Sequences. *Statistical Science* 7:457–511.

- Hornocker, M. G. 1969. Winter Territoriality in Mountain Lions. *The Journal of Wildlife Management* 33:457–464.
- Karanth, K. U. 1995. Estimating tiger *Panthera tigris* populations from camera-trap data using capture-recapture models. *Biological Conservation* 71:333–338.
- Karanth, K. U., and J. D. Nichols. 1998. Estimation of Tiger Densities in India using photographic captures and recaptures. *Ecology* 79(8):2852–2862.
- Moeller, A. K., P. M. Lukacs, and J. S. Horne. 2018. Three novel methods to estimate abundance of unmarked animals using remote cameras. *Ecosphere* 9:e02331.
- Montana Fish Wildlife and Parks. 2019. Montana mountain lion monitoring and management strategy.
- O’Connell, A. F., J. D. Nichols, and K. U. Karanth. 2011. Camera Traps in Animal Ecology : Methods and Analyses. Page (A. F. OConnell, J. D. Nichols, and K. U. Karanth, Eds.). Springer.
- Paterson, J. T., K. Proffitt, B. Jimenez, J. Rotella, and R. Garrott. 2019. Simulation-based validation of spatial capture-recapture models: A case study using mountain lions. *PLoS ONE* 14:1–20.
- Plummer, M. 2017. JAGS: Just Another Gibbs Sampler.
- Plummer, M., A. Stukalov, and M. Denwood. 2019. rjags.
- Proffitt, K. M., J. G. Goldberg, M. Hebblewhite, R. Russell, B. Jimenez, H. S. Robinson, K. Pilgrim, and M. K. Schwartz. 2015. Integrating resource selection and harvest into spatial capture-recapture models for large carnivores. *Ecosphere* 6.
- Rowcliffe, J. M., J. Field, S. T. Turvey, and C. Carbone. 2008. Estimating animal density using camera traps without the need for individual recognition. *Journal of Applied Ecology*

45:1228–1236.

Royle, J. A., K. U. Karanth, A. M. Gopaldaswamy, and N. S. Kumar. 2009. Bayesian inference in camera trapping studies for a class of spatial capture-recapture models. *Ecology* 90:3233–3244.

Royle, J. A., and K. V Young. 2008. A hierarchical model for spatial capture-recapture data. *Ecology* 89:2281–2289.

Russell, R. E., J. A. Royle, R. DeSimone, M. K. Schwartz, V. L. Edwards, K. P. Pilgrim, and K. S. McKelvey. 2012. Estimating abundance of mountain lions from unstructured spatial sampling. *Journal of Wildlife Management* 76:1551–1561.

Seidensticker, J. C., M. G. Hornocker, W. V Wiles, and J. P. Messick. 1973. Mountain lion social organization in the Idaho Primitive Area. *Wildlife Monographs* 35:3–60.

Team, R. C. 2019. R: A Language and Environment for Statistical Computing. Vienna, Austria.